Shape of adsorbed supercoiled plasmids: An equilibrium description

Nam-Kyung Lee,[1] Tatiana Schmatko,[2] P. Muller,[2] M. Maaloum,[2] and A. Johner[2]
[1]*Institute of Fundamental Physics, Department of Physics, Sejong University, Seoul 143-743, South Korea*
[2]*Institut Charles Sadron, CNRS-UdS, 23 Rue du Loess, BP 84047, 67034 Strasbourg cedex 2, France*
(Received 9 November 2011; published 22 May 2012)

Inspired by recent atomic force microscope (AFM) images of plasmids deposited on oppositely charged supported lipid bilayers from salt free solution, we propose a model for strongly adsorbed supercoiled cyclic stiff polyelectrolytes. We discuss how the excess linking number Lk of the deposited cycle is shared between writhe Wr and twist Tw at equilibrium and obtain the typical number of self-crossings in the deposited cycle as a function of surface charge density. The number of crossings at equilibrium is simply determined by the crossing penalty which is a local quantity and by the excess linking number. The number of crossings is well defined despite versatile plasmid shapes. For moderate numbers of crossings the loops are rather small and localized along the primary cycle, as expected from entropic loops. In the regime of many crossings, the cycle takes the shape of a regular flat ply ruled by local stiffness. The model allows for a semiquantitative comparison with the AFM images of deposited plasmids which are strongly charged.

DOI: 10.1103/PhysRevE.85.051804 PACS number(s): 87.14.gn, 87.15.ad, 87.15.hp

I. INTRODUCTION

Double stranded DNA (hereafter dDNA) outside of nucleosomes are widespread in nature from bacteria to eukaryotic cells. They are generically called plasmids and are often circular, as considered here. Plasmids are intensively studied and used to transfer genetic material. Historically they served to create rat genetic disease models, nowadays they are promising vectors in gene therapy. Large plasmids as used in the experiments performed by some of us [1] comprise 2686 base pairs and make a contour length S of about 900 nm. As dDNA in general, plasmids carry one (negative) elementary charge e per base and are highly charged objects subject to charge regulation. Being closed cycles, plasmids can bear some extra turns which would be released upon opening the cycle: Plasmids are supercoiled objects. The number of trapped extra turns can to some extent be controlled during the preparation, of order ten (negative) extra turns is typical. A sketch of plasmid structure in solution and deposited on a surface is given in Fig. 1.

Supercoiling in general got a lot of attention from physicists [2], especially from the single chain manipulation community [3,4]. When open dDNA molecules moderately stretched in a magnetic (or optical) tweezers are subjected to extra turns the formation of plectoneme is detected [4]. Plectoneme is a "phone cable" -like supercoiled structure of dDNA in equilibrium with the stretched strands [see Fig. 1(c)] [5]. Modeling of supercoiled structures is proposed by very different communities ranging from mechanics [6,7] to statistical physics [8,9] including computer simulations [10–12]. The fascination of theorists for closed dDNA comes in part from the conservation of the link Lk and the various ways it can be shared between writhe Wr and twist Tw. For a comprehensive review, see Ref. [5]. The typical configuration in solution has nonvanishing writhe and goes hence out of plane. In contrast, the deposited plasmids are constrained to be planar almost everywhere by the strong surface attraction and writhe only comes from the self-crossings. In a full statistical physics model, each plasmid configuration having the proper link is Boltzmann weighted with an elastic energy comprising the bending (E_b) and twist (E_t) contributions [8]. The elasticity of dDNA is generally described by a bending modulus $B = k_B T l_p$ with l_p the persistence length and a twist modulus $C = k_B T l_t$ with l_t the twist length. In principle, the handedness of dDNA allows a linear coupling between twist and curvature [13]. However, this coupling is too weak to enter our current description. The elastic moduli depend on external conditions such as ionic strength. Electrostatic stiffening in dilute bulk solution is described by the Odijk-Skolnick-Fixman theory [14], which leads to the simple dependence $l_p = l_{p0} + l_B \rho^2 \kappa^{-2}/4$, where κ^{-1} is the Debye screening length decreasing for increasing ionic strength, as discussed later, $l_B = e^2/4\pi\epsilon k_B T$ is the Bjerrum length, about 0.7 nm in water, and ρ the linear charge density. At high ionic strength $l_p = l_{p0} = 50$ nm. Below we use thermal units where elementary charge is set $e = 1$.

Even *in vitro*, most studies on plasmids are conducted under physiological conditions where the ionic strength is as high as 0.15 mol/l. One obvious reason is to ensure biological relevance. Going to low salt could also lead to denaturation of the dDNA, which usually is not desired. From the theoretical point of view the status of electrostatics at high salt remains unclear in part because the relevant distances are very short and the mean field theories like Poisson-Boltzmann theory fail. For long the electrostatic interactions are neglected altogether or represented by some *ad hoc* short range interaction. Recently there were attempts to include electrostatics in the description of plectoneme [15]. The Poisson-Boltzmann equation in the presence of (moderate) salt has only recently been solved analytically in cylindrical geometry [16]. This substantiates the concept of effective charge often used to extend the validity of the linear Debye-Hückel theory.

Plasmids away from physiological conditions are also interesting objects for the physicist because of their versatile structure. In solution, the shape (structure) of a (cyclic) plasmid mainly depends on its supercoil density and on salt conditions ruling electrostatics. In practice the polarization of the dissolved salt at concentration c_s entails the Debye screening length κ^{-1} for electrostatics with $\kappa^2 = 8\pi l_B c_s$ (for monovalent salt). In solution the effective interaction between

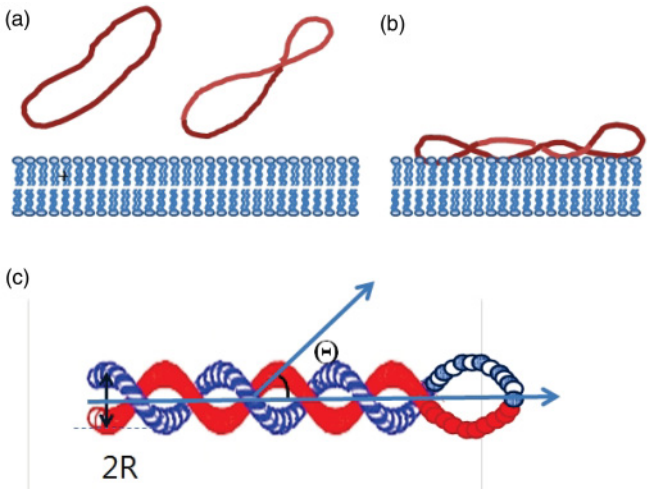

FIG. 1. (Color online) Sketch of plasmids (a) in bulk solution and (b) deposited on a planar membrane. (c) Supercoiled DNA: plectonemic structure with a helical angle Θ and a helical radius R.

test charges is cut exponentially over the Debye screening length. The underlying Debye-Hückel theory is a linear theory which is often used for polyelectrolytes sometimes together with the concept of effective charges mentioned earlier. Qualitatively we expect the isolated plasmid in (almost) salt free solution to be ruled by bare electrostatics and to adopt an almost planar stretched configuration thereby almost all extra link is stored into twist. In the opposite limit of strong screening (high salt) the electrostatic interaction becomes a short range repulsion which is not very relevant for intrinsically stiff plasmids (with persistence length $l_p \sim 50$ nm). The plasmid can then adopt a ply structure where most of the link is stored into writhe and the stiff plasmid mainly pays curvature (bending) energy [17]. The ply structure is documented by a host of electron micrographs; these images are routinely used to compute the excess linking number of plasmids [18]. Intermediate situations deserve more precise consideration.

It is not that easy to adsorb the negatively charged plasmids (more generally DNA) from aqueous solution because substrates usually also acquire a negative charge when they are brought in contact with water. An often used trick is to fix the DNA on the substrate using divalent cations (Mg^{2+}). In a recent work Witz *et al*. [19,20] show that under those circumstances a plasmid behaves as locally stiff over the first few persistence lengths (say five) and like a two-dimensional (2D) excluded volume chain at somewhat larger distances (say above seven persistence lengths). We expect a similar behavior to hold for somewhat softer adsorption as is the case in our experiments. In plasmid deposition experiments performed by some of us [1] the surface is a supported lipid mixed bilayer. The nominal surface charge concentration is controlled by the fraction of charged lipids versus neutral (yet zwitterionic) ones. We do not fully address peculiarities of such a substrate like its possible inhomogeneity (in the absence of plasmid) and the possible formation of cationic lipid/DNA complexes. In all examined cases the plasmid lies flat on the surface and in that sense it is "strongly adsorbed" without any sign of denaturation. We actually checked with UV adsorption measurements that even in the salt free solution at the same plasmid concentration there

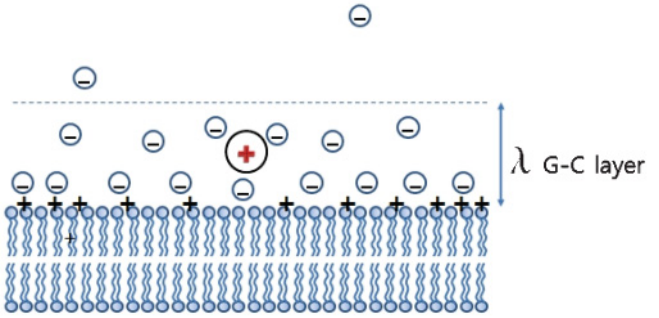

FIG. 2. (Color online) Displacement of mobile surface charges and bulk charges due to the presence of a test charge near the interface.

is no sign of double helix melting over more than 10 h at room temperature. In contrast complete melting is observed over a few tens of minutes at 80° C. Open DNA fragments are seen to melt much easier than plasmids. Furthermore, as we report below the recorded shapes are similar to those of plasmids deposited on a neutral (dipolar) surface from a solution with tens of mM monovalent salt. In the later case DNA melting is not expected.

The main remaining question is to describe the adopted plasmid shape which can be characterized by its number of self-crossings. This is the main purpose of the present paper. The shape after deposition from a (almost) salt free solution depends on the surface charge density as also demonstrated by experiment. We show below that the surface charge for a deposited plasmid stands in a loose analogy with the salt concentration for a plasmid in solution. The water-lipids interface is polarizable because the ionic cloud of counterions above the charged surface and the surface charges themselves if they are mobile or the counterions trapped by the surface in the strong coupling limit (yet without ion pairing or strong in-plane correlations) can all be slightly displaced by a test charge (see Fig. 2). We expect electrostatic interactions to be screened due to the mobile charges. However, since only the interface of limited thickness is polarizable, the tail of the effective interaction decays only as a (high) power law [21], in contrast to the free solution case where an exponential decrease is predicted.

We try to describe supercoiled stiff cycles with prescribed excess link Lk deposited from salt free solution and salty solution on a charged or polar (zwitterionic) surface. The excess link Lk is a topological invariant for a closed cycle; it is the sum of the twist Tw and the writhe Wr,

$$\mathrm{Lk} = \mathrm{Tw} + \mathrm{Wr}. \tag{1}$$

Under given external conditions, the cycle can adapt its conformation to minimize the free energy with conserved link Lk. When the external conditions are changed, twist may be traded against writhe or vice versa. In the remainder we focus on cycles adsorbed on a oppositely charged surface. We merely consider cycles with given uniform charge density ρ and persistence length l_p. Only in the final discussion do we try to comment on the variation of ρ and l_p with the surface charge. Below we present precise analytical results obtained in some linear approximation [22] which allow a semiquantitative comparison with adsorbed plasmids.

II. PLASMID DEPOSITED ON AN OPPOSITELY CHARGED SURFACE

In this section we consider the self-crossing of a plasmid adsorbed on the oppositely charged surface. The cross section of a crossing is illustrated in Fig. 3. Below, we first estimate the extension of the polymer sections not touching the surface around crossings and show that crossings have only localized effect. Another energy penalty arises from the mutual interaction of electrostatic origin between (straight) polymers at crossings and is of the type $F_{\rm int} = \text{const.}/\sin\theta$, with θ the angle of crossing and an amplitude estimated from perturbation theory. Then we estimate the writhe in the case of a plasmid lying flat on the surface almost everywhere. With these estimates at hand, we finally discuss the free energy of the cycle as a function of the number of crossings.

A. Interactions near charged surface

Let us first consider a surface with a uniform (continuous) quenched positive surface charge and assume infinite dielectric contrast, as is reasonable for an aqueous solution facing a low dielectric substrate. Whether the fluctuations are important depends on the coupling parameter $\Xi = 2\pi Z^3 l_B^2 \sigma$, where σ is the surface charge density and Z the valency of the surface charge counterions [23]. For $\Xi < 1$, the layer of counterions can be described by the mean-field theory (Gouy-Chapman). For monovalent surface charges ($Z = 1$), $\Xi = 1$ corresponds to an average distance $\sqrt{2\pi} l_B$ between surface charges. In the experiment the charged surface is a bilayer with a fraction of monovalent charged surfactants which corresponds typically to $\Xi \lesssim 1$. As the coupling constant Ξ is rapidly increasing with Z we specialize our mean-field description to $Z = 1$ below, as is also relevant to experiment [1].

In the mean-field theory, half of the counterions of the interface are (qualitatively) spread within a Gouy-Chapman

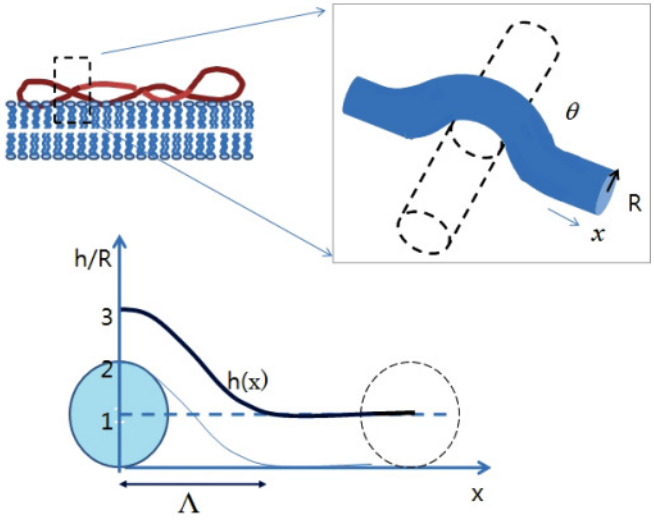

FIG. 3. (Color online) A self-crossing of plasmid under strongly adsorbing condition. The centerline of upper filament is described by $h(x)$. For each crossing, there is some polymer section not touching the surface which costs interaction energy; the upper strand bends back to the surface at the expense of elastic energy.

(GC) length $\lambda = \frac{1}{2\pi\sigma l_B}$ from the surface. The coupling constant Ξ measures the strength of the Coulomb interaction between two typical charges in the GC layer a distance λ apart. In the case $\Xi > 1$, the counterions condense on the surface until the GC length goes back to l_B. For valencies larger than unity, the counterions are also expected to be ordered in the surface [23, 24]. Strong coupling results with emphasis on overcharging are reviewed by Grosberg *et al.* [25] and Messina [26]. Lukatsky *et al.* [27] and Lau *et al.* [28] also address correlation effects in simple geometries.

Interactions between test charges immersed in the GC layer are weakly screened. A test charge polarizes the surrounding layer creating a dipole, the potential created by such a dipole is not strongly screened because most relevant field lines stay essentially out of the GC layer, in a region where counterions are scarce. As a result the effective interaction ψ between unit test charges (located at the same height, z) decays with lateral distance r as a power law. The case of no dielectric contrast at the interface was considered in detail by Netz [22]. The perturbation of the electric potential by a unit source charge (Green's function) reveals a very complex behavior. Most strikingly, for a source charge and a test point at the same height within the GC layer the perturbation decays with the distance r as a power law $\psi(z,r) = \frac{2l_B\lambda^2}{r^3}$ $(z < \lambda, r > \lambda)$ [22]. The power-law tail is given by the leading nonanalytic term of the low-q expansion of $\psi(z,q)$, with $\mathbf{q}$ being the conjugate variable of $\mathbf{r}$ (see Appendix B).

Using linear perturbation of GC solution, we derive interactions near charged surface for other experimentally relevant cases. The detailed calculation is shown in Appendix B. To account for the experimental situation of plasmids adsorbed on a lipid bilayer in the fluid gel phase we considered high dielectric contrast and annealed surface charges. In the case of infinite dielectric contrast and a quenched surface charge [denoted below by superscript (q)], we obtain a slightly stronger power law decrease right at the interface ($z = z_0 = 0$), $\psi^{(q)}(0,r) = \frac{18 l_B \lambda^4}{r^5}$ $(r > \lambda)$. It is worth noticing that a finite (yet large) dielectric contrast restores the $1/r^3$ behavior [22] with an amplitude divided by the dielectric contrast (the ratio of dielectric constants, here of order 20). The true asymptotics remains formally $\sim 1/r^3$. In the case of a annealed surface charge [denoted below by superscript (a)] the electrostatic potential at the surface of the substrate is nonuniform and the surface charge is Boltzmann distributed. We find that the amplitude of $\psi^{(a)}$ is smaller by a factor 9 as compared to the quenched case $\psi^{(q)}$:

$$\psi^{(a)}(0,r) = \frac{2 l_B \lambda^4}{r^5} \quad (r > \lambda). \tag{2}$$

The detailed derivation can be found in Appendix B. We also provide details on the interaction between the source at height z_0 and a test charge at height z, $\psi(z,r) = G(z,r)$, for various relevant cases. In the annealed case the surface charge is Boltzmann distributed following $\sigma = \sigma_0 e^{-\psi}$, where σ_0 is the nominal surface charge density measured at the unperturbed surface infinitely far from the source. In the linear regime we may compute $\delta\sigma = \sigma - \sigma_0$ as $\delta\sigma(q) = -\psi(z_0,0,q)/(2\pi l_B)$, an explicit expression can be obtained with the help of Appendix B 3. The total excess charge induced by a unit test

charge located at height z_0 can be computed by setting $q = 0$:

$$\delta\sigma(q=0) = -\frac{2}{3}\frac{\lambda}{z_0+\lambda}. \quad (3)$$

A rod of charge ρ per unit length accumulates $-2\rho/3$ extra surface charges per unit length underneath. This excess surface charge partially compensates the image charge. The second moment of the surface charge distribution shows that the width of the perturbation crosses over from $\sim\lambda$ for $z_0 < \lambda$ to $\sim z_0$ for $z > \lambda$. This suggests that the perturbation starts failing for $\rho 2\pi l_B \sim 1$ for a filament close to the substrate.

Note that the efficiency of (any) screening depends on the spatial dimension of the charged object. Screening only marginally affects a 1D slender object like a rigid rod. In the absence of salt (which is not realistic) the GC description leads to an infinite electrostatic potential difference between the surface and infinitely far away. Indeed, if the origin of the potential is taken at the surface, the electrostatic potential at distance z away from the surface can be written as $\varphi(z) = -2\ln\frac{z+\lambda}{\lambda}$. The volume charge density of the counterions decays from $c(0) = -\sigma/\lambda = -2\pi l_B\sigma^2$ as $c(z) = c(0)(\frac{\lambda}{z+\lambda})^2$. The concentration of counterions is essentially constant in the GC layer and decays as a power law further from the surface. A small quantity of otherwise irrelevant (negatively charged) coions of the surface are depleted following the inverse Boltzmann law. In the absence of any bulk screening, none of them would be found at a finite distance from the bilayer. In practice, there is some screening in the bulk solution due in our case to the finite concentration of plasmids and their counterions. The salt at infinity is composed of condensed plasmids bearing a high effective charge ($\sim -1000e$) and their monovalent free counterions. Due to the high valency of plasmids, a naive Debye-Hückel (DH) formula would lead to a very short estimate of the screening length. The DH screening volume would typically not contain any plasmid. The relevant screening length is hence the average distance between plasmids (or the DH length due to water dissociation, whichever is shortest). Due to the bulk screening, the electrostatic potential does no longer diverge but saturates at a few screening lengths from the surface $\varphi(\infty) = 2\ln\frac{\kappa\lambda}{2}$ for ($\kappa\lambda \ll 1$). For a comprehensive presentation of the GC theory, see the book by Safran [29].

In the case of bilayers in the fluid phase and in the so-called gel phase, the surface charges are free to diffuse and rearrange. In this sense the surface charge is annealed [30,31] and this allows additional polarization effects. The image charge (here of the same sign as the test charge) favors counterion condensation (localization). On the other hand, the surface charge attracts the plasmid and repels its counterions, resulting in counterion release. These competing effects are considered in Ref. [32] for a charged rod. A discussion of charge regularization and effective linear charge density is postponed to Sec. III.

B. Crossings: Filaments shape and relative orientation

When a circular DNA is adsorbed on the membrane and adopts a configuration with nonvanishing writhe, there are approximately as many crossings as the writhe. At a given crossing, we may define an upper strand and a lower strand. One strand passes over the other strand lying flat on the surface (see Fig. 3). The shape of the filament at crossings results from the interplay between the interaction of the upper filament with the surface, the bending energy of the upper filament, and the interaction between the two crossing filaments. The latter could lead the upper filament to float over the lower one without contact. The mutual interaction between two crossing lines near the charged surface is not singular. Without any screening the (Coulomb) interaction would be singular for infinite lines but the energy gain ΔE when displacing one line to the height h is regular and only linear in h. With right angle crossings, $\Delta E = l_B\rho^2\int_{-\infty}^{\infty}\{\frac{-1}{\sqrt{x^2+y^2+h^2}} + \frac{1}{\sqrt{x^2+y^2}}\}dxdy = 2\pi l_B\rho^2 h$. This means that the difference in interaction energy is dominated by a small section of the filaments within a distance h from the crossing. Provided the characteristic length Λ of the sought profile of the upper filament is larger than h, the interaction energy with the reference taken at $z = 0$ will depend on h only and is independent of the profile of the upper filament in first approximation. The associated interaction between filaments may hence be represented by a repulsive point force $f_{1\to 2} = 2\pi l_B\rho^2$ acting on the upper filament right at the crossing. Relying on the separation of scales, we may hence solve for the profile with the filament interaction entering through the boundary condition only and calculate the floating height h (yet $h \ll \Lambda$). We may also consider the case where the upper filament is not floating but in contact (as seems to be the case in experiments); the lower filament then exerts a contact force (against interpenetration) on the upper one. Contact is preserved as long as the repulsive force between filaments does not cancel the contact force. This will determine the minimum surface charge ensuring contact in a purely mechanical picture (without thermal fluctuations). The Green's functions given in Appendix B do also allow to access the self-energy of the rods (in the linear perturbation), which depends on the distance to the surface. The image charge effect entails a logarithmic divergence of the self-energy when the height of the filament vanishes. Considering electrostatics alone, the current approximation predicts filaments to float over the surface [32], less so for annealed surface charge. In Sec. III B we argue, following Ref. [32], that due to the induced extra surface charge self-energies cancel to a large extend for strongly charged filaments. The adsorption of strongly charged plasmids on the annealed bilayer is then primarily ruled by the interaction with the surface charge. According to Ref. [32], this holds true for strongly charged filaments and annealed surface charges, albeit counterion release takes place and charge densities need to be renormalized. The calculation presented below considers only direct interactions of the upper filament with the lower filament and with the surface charge.

1. Filament shape

The aim of this paragraph is to show that the deformation of the upper filament is localized and that the associated penalty increases with the surface charge in the weak coupling limit ($\Xi < 1$). The mutual in-plane interaction, to be calculated later, will turn out to dominate and to determine the number of self-crossings over most of the regime $\Xi < 1$.

Here we assume that the upper filament is in contact with the lower filament which is flat on the surface. The shape of the upper filament is assumed to be described by that of its central line. Let $h(x)$ be the out-of-plane deflection of the upper filament central line near a crossing as shown in Fig. 3. The strong attraction to the surface by the linearized GC potential $\varphi(h) = 2h/\lambda$ constrains the filament to be on the substrate but at crossings. The shape of the filament at crossings is minimizing the free energy functional $F[h(x)] = \int l_p(h''(x))^2 dx/2 + \int 2\rho h(x)/\lambda dx$. The Euler Lagrange equation for $h(x)$ reads $l_p h^{(4)} + 2\rho/\lambda = 0$. The upper strand starts parallel to the surface at height $z = 3R$. Let us consider the upper strand to be of finite length. For a strong enough field, it touches the surface with a finite angle. For a well defined, somewhat higher attraction, the contact angle vanishes. For even higher attraction the outermost part of the filament just lies flat on the surface. This is the regime of interest here. The function $h(x)$ hence vanishes at a finite distance Λ from the crossing and $h'(\Lambda) = 0$, $h''(\Lambda) = 0$. Integrating the Euler-Lagrange equation we obtain the profile

$$\frac{h(x)}{R} = -6\left(\frac{x}{\Lambda}\right)^4 + 16\left(\frac{x}{\Lambda}\right)^3 - 12\left(\frac{x}{\Lambda}\right)^2 + 3, \qquad (4)$$

$$\text{with} \quad \Lambda^4 = 72\frac{R\lambda l_p}{\rho}. \qquad (5)$$

Integrating up the penalty for going out of plane at the crossing we obtain the optimal value of $F[h(x)]$, $F_h = \frac{64}{15}\frac{\rho R\Lambda}{\lambda}$. This contribution is decreasing with λ as $F_h \sim \lambda^{-3/4}$ [in case of counterion condensation/release there is also some dependence on λ (σ) hidden in ρ].

In the experiments plasmids lie (almost) flat even on neutral (dipolar) supported bilayers. This we attribute to some short range interaction with the substrate not taken into account above. Let μ be the associated gain of free energy per unit length touching the surface, a simple scaling argument balancing the bending energy $l_p R^2/\Lambda^4$ and the contact energy $\mu\Lambda$ gives $\Lambda^4_{\text{local}} \sim l_p R^2/\mu$. It was implicitly assumed in Eq. (5) that $\mu < \rho R/\lambda$ for the charged surfaces of interest. In the following we use the fact that deformations out of plane at crossings are very localized compared to the size of the small flat loops.

The obtained shape makes sense if the curvature of the upper filament at the crossing is smaller than $1/2R$ for right angle crossing (otherwise the upper filament has to wrap around the lower one). This condition is fulfilled in experiments due to the large value of l_p, which is the only true large scale in practice. The derivatives of free energy functional $F(h)$ with respect to h gives the force f required to sustain the shape of the upper filament we obtain $f = 2l_p h^{(3)}(x = 0)$.[1] This force should be the sum of the repulsive force $f_{1\to 2}$ given earlier and the contact force $n_{1\to 2}$ exerted by the lower filament on the upper one. By this force balance, we obtain $n_{1\to 2} = 2l_p h^{(3)}(x = 0) - f_{1\to 2}$. From the condition that the contact force is repulsive (acts against interpenetration) and vanishes in the marginal case, the force balance gives the criterion $\frac{\lambda^3 l_B^4 \rho^5}{R l_p} \lesssim 1$ for not floating. The criterion is satisfied whenever the surface charge is high enough to observe crossings.

[1] Alternatively one can calculate the energy of the filament as a function of $h(0)$ and take its derivative. To do so it is enough to replace R with $(h(0) - R)/2$ in the expressions of Λ and F_h.

2. *In-plane interaction between filaments at crossings*

Let us assume that two filaments (the projections of their central lines on the substrate) cross with a finite angle θ. Because the interaction between projections is decaying fast $\sim 1/r^3$ at large distances ($r > \lambda$), we expect that the projections can be approximated by infinite straight lines and further put all charge on the central line. The interaction between straight infinite filaments parallel to the surface can be written in the form of $F_{\text{int}} = V(q = 0,z)/\sin[\theta]$, where $V(q = 0,z)$ is the Fourier transform of the potential $V(x,y,z)$ with respect to the in-plane coordinates x,y (see Appendix A for details). This expression holds provided the integral of $V(x,y,z)$ over the in-plane coordinates x,y is convergent. The $\sin\theta$ in denominator indicates that the filaments prefer to be perpendicular at crossings (for repulsive potential V). As the potential $V(q,z)$ is known perturbatively in various cases, we get explicit results for the interaction. The interaction is calculated in the very vicinity of the surface $z \approx 0$. Calculating the potential as a linear perturbation to the GC solution (see Appendix B 3) yields for a quenched surface charge $V(q = 0) = 4\pi l_B \lambda \rho^2$ and we finally obtain $F^{(q)}_{\text{int}} = \frac{4\pi l_B \rho^2 \lambda}{\sin\theta}$ (again a dependence on λ is hidden in ρ). This expression can be justified because at the crossing the projections change sign of curvature and are hence locally straight. The same method can be used in other more relevant situations. If the surface charge is annealed and hence participates in the screening the interaction is reduced by a factor of 3 (right at the surface), we obtain $F^{(a)}_{\text{int}} = \frac{4\pi l_B \rho^2 \lambda}{3\sin\theta}$. This shows that the surface charge screens more efficiently than the diffuse countercharge in the GC layer. One can also go to the very limit of a 2D plasma with charge densities σ_+, σ_- for cations and anions respectively (Appendix B 2). The surface charge vanishes in total but can be polarized. The interaction energy is then weaker $F^{(pl)}_{\text{int}} = \frac{2\pi l_B \rho^2 \lambda^\star}{\sin\theta}$, with $\lambda^\star = 1/(2\pi l_B(\sigma_+ + \sigma_-))$. If only the counterions localized on the surface (of density σ_-) are mobile, σ_+ must be set to zero. These results are consistent with the fact that the screening surface charge densities combine linearly in the interaction. The diffuse GC charge counts half as much as the localized (polarizable) surface charge. This in-plane interaction turns out to rule over crossings; in summary,

$$F^{(q)}_{\text{int}} = \frac{4\pi l_B \rho^2 \lambda}{\sin\theta}, \quad F^{(a)}_{\text{int}} = \frac{4\pi l_B \rho^2 \lambda}{3\sin\theta}, \quad F^{(pl)}_{\text{int}} = \frac{2\pi l_B \rho^2 \lambda^\star}{\sin\theta}, \qquad (6)$$

where the superscripts (q), (a), and (pl) stand for quenched, annealed, and plasma, respectively.

In the case of a neutral surface (discarding possible surface dipoles) and in the presence of salt entailing a Debye length κ^{-1}, we obtain $F_{\text{int}} = \frac{4\pi l_B \rho^2 \kappa^{-1}}{\sin\theta}$, right at the surface (see Appendix B 1). This is twice larger than obtained naively from the bulk Yukawa potential $l_B \exp -\kappa r/r$, when the interacting charged lines are entirely surrounded by salt, in the bulk or infinitely away from the surface.

These simple values are obtained for charged lines very close to the surface; a little bit away from the surface there is

a power law correction in the reduce distance z/l_{ch}, with the characteristic length l_{ch} being, λ, $\lambda^\star$, or κ^{-1}, respectively.

These estimates rely on the linear perturbation of the GC layer and of the surface charge by a test charge. In this sense they are of the DH type. In Sec. III B, we argue that the expression for the interaction remains valid with a renormalized linear charge density. The latter results from the competition between many effects (charge regularization, counterion release, image charge, depletion of plasmid charge at crossings) but remains of order $\sim 1/l_B$ (the bare plasmid charge is about $4/l_B$).

C. Writhe

We are mainly concerned with the calculation of the writhe of the adsorbed plasmid. In general writhe can be calculated by averaging directed writhe over all projections on planes. For a projection the directed writhe is the sum of the signed crossings [5]. If the configuration is almost in a plane $\mathcal{P}$, the writhe is close to the directed writhe Wr_{pr} of the projection on $\mathcal{P}$. In other words, the writhe is close to 1 (-1) per crossing. In general, there is nothing like a writhe density which could be integrated along the plasmid contour. However, the difference of writhe with respect to a close reference shape can be (under rather soft conditions) expressed as an integral along the reference contour [33]. In our case the reference contour is the projection on the surface (corresponding to the plane $\mathcal{P}$). An upper bound for the error when counting writhe unity per crossing can be written as $|\mathrm{Wr}-\mathrm{Wr}_{pr}| \leqslant \frac{1}{2\pi}(1-(\frac{S_{pr}}{S})^2)^{1/2}(S_{pr}\int C_{pr}^2 \mathrm{d}s_{pr})^{1/2}$. The integral is running over the projected contour of total length S_{pr} and local curvature C_{pr}. In our case the configuration is, ideally, taken to be in the substrate plane everywhere but in a region of extension Λ near crossings. A rough (over) estimate is obtained by further replacing Λ with the DNA radius R, $\frac{|\mathrm{Wr}-\mathrm{Wr}_{pr}|}{n} < \frac{\theta}{\pi}\sqrt{\frac{R}{S/n}}$. Here n is the number of crossings and S the plasmid contour length, the large aspect ratio of the plasmid (actually of the strand between crossings) makes the error negligible.

D. Equilibrium shape of the plasmid

As explained earlier, supercoiling at the surface which results in self-crossings converts some of the twist initially stored in the stretched cycle into writhe. Thereby, the elastic twisting energy is reduced. At the same time, crossings cost energy, some due to the loss of attractive interaction with the surface, some due to the repulsive interaction between filaments. Some extra elastic in-plane bending energy is generally not dominant. Another slight complication arises because at crossings the dDNA goes out of the surface and the centerline of the filament can twist. A more general discussion of the total energy is provided in Appendix C.

Here we give a simplified discussion designed to be physically transparent. The main contributions to the energy are the penalty for crossings and the twisting energy. Because each crossing takes away one turn of twist the total twist is $\mathrm{Tw} = \mathrm{Lk} - n$. The twist is distributed over the majority length lying flat on the surface, where it is stored as material frame twist and the small sections involved in crossings. As the filament goes out of plane at crossings and the osculatory plane turns by a finite angle there is high centerline twist which has to be compensated by material frame twist to avoid extra energy penalty. As a consequence, the twist is thought to be uniformly distributed along the plasmid. The twist energy can hence by approximated as $E_t = l_t 2\pi^2(\mathrm{Lk}-n)^2/S$. The penalty for crossing has two main contributions: the interaction with the surface F_h and the interaction energy between filaments F_{int}. Retaining only these terms leads to the total energy $F = l_t 2\pi^2(\mathrm{Lk}-n)^2/S + n(F_h + F_{\mathrm{int}})$. Optimizing this simplified energy with respect to the number of crossings n results in a first approximation to a linear decrease of the number of crossings with the penalty for a crossing:

$$\mathrm{Lk} - n = \frac{S}{4\pi^2 l_t}(F_h + F_{\mathrm{int}}), \tag{7}$$

where a weak dependence of F_{int} on n through crossing angle θ has been neglected. The simple expression Eq. (7) merely relies on the fact that the penalty for a crossing is local, not sensitive to the overall shape. This feature is expected to be rather robust and we can exploit it without further modeling. Knowing the plasmid length S and twist length l_t a measure of n gives direct access to the total penalty for a crossing under the given conditions. Assuming $l_t = 70$ nm and $S = 900$ nm, the data correspond to a penalty for crossing of $11k_BT$ and $16k_BT$ for the area per surface charge 4 nm^2 and 6 nm^2, respectively. We show later that these values correspond to effective filament charges of order $\sim 1/l_B$, as expected. Let us first comment on how F_h and F_{int} vary with experimental parameters.

At low surface charge, the right hand side of Eq. (7) is dominated by F_{int} (in practice until close to the strong coupling regime), which is a decreasing function of the surface charge. At somewhat higher surface charge, it is dominated by F_h, which increases with the surface charge. We hence predict a nonmonotonic variation of the number of crossings with the surface charge in the weak GC regime of the surface.

When the nominal surface charge exceeds $1/(2\pi l_B^2)$, the surface charge is regularized and the unperturbed interaction of the filament with the surface is almost constant. On the other hand, as more and more ions are localized in the interface (and actually at the surface), the interaction between filaments at crossings is now even more strongly decreasing with the surface charge than in the GC regime and a steep upturn of the number of crossings is expected. If it comes to stable Bjerrum pairing [34], which certainly depends on chemical details, the polarizability of the interface only slightly increases with its nominal charge and sharp upturn is no longer expected.

In a regime of low surface charge, only a few crossings are expected. Let us assume that the contour length is distributed evenly over the flat projected loops. The resulting loops would be large and essentially flexible because the surface screening is enough to avoid a dramatic electrostatic stiffening. Consider, for example, a figure eight consisting of two equal size loops in a flexible cycle. As it is unstable, the cycle will be partitioned between the smallest possible loop and its large complement [35,36]. The reason for localization is the strongly singular return probability in 2D self-avoiding statistics and the large vertex exponent $\sigma_4 = -19/16$ (as any further crossing is forbidden the projection is treated as self-avoiding) [36]. In our case the smallest thermal loop [19] corresponds to about the

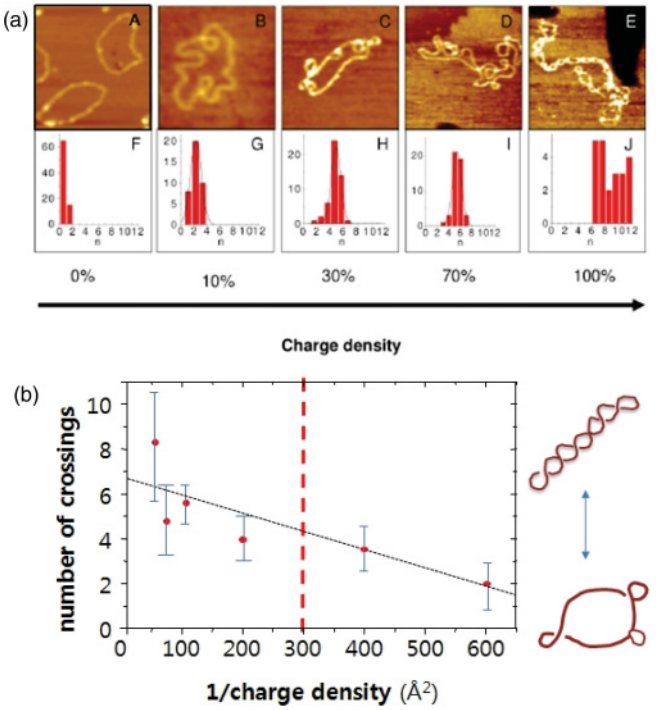

FIG. 4. (Color online) (a) Typical AFM images (A)–(E) of adsorbed plasmid on lipid bilayers. The fraction of cationic lipids grows from 0 to 100%, as indicated. The distributions of the number of crossings measured under given surface charge density are shown below (F)–(J). (b) Experimentally measured average number of crossings as a function of inverse surface charge density. Error bars indicate the width of measured distribution. The straight line represents the linear regime predicted by Eq. (8) for low surface charge ($\Xi < 1$). The dashed vertical line indicates the border between weak and strong electrostatic coupling of the interface ($\Xi = 1$). The extrapolation of the linear regime to high surface charge determines the extra link $\mathrm{Lk} = (-)7$ confirmed by electrophoresis. The extrapolation to zero crossings makes it possible then to asses the effective plasmid charge (near crossings) in the moderate surface charge regime.

persistence length l_p. The overall shape of the plasmid is hence a large loop decorated with small loops about one persistence length in size (see Fig. 4). The electrostatic interaction at crossings imposes right angle crossings.

At higher surface charge, there are more crossings and an evenly distributed contour length leads to (short) stiff loops. We hence expect a regular arrangement in an array of equal-sized loops which we could call an open (as opposed to tight) ply. In this regime the angle at crossing is somewhat smaller because bending energy is competing with the direct interaction at crossings. Recorded atomic force microscope (AFM) images in Fig. 4 show that the variation of the plasmid shape with the surface charge agrees with our expectations (for experimental details and more data, see [1]). The measured average of the number of crossings n taken over many images [Fig. 4(b)] displays the predicted nonmonotonic behavior (despite the error bars). It is tempting to exploit the "linear" variation of the number of self-crossings with the area per surface charge at moderate surface charge. In this regime we recast the number of crossings n as

$$n = \mathrm{Lk}\left(1 - \frac{\sigma_0}{\sigma}\right), \qquad \text{with} \quad \sigma_0 = \frac{S}{6\pi^2 \mathrm{Lk} l_t}\rho^2. \tag{8}$$

The suggested linear law supposes that the effective charge density ρ has a smooth variation with σ in this regime. The straight line extrapolates to a value $\bar{\mathrm{Lk}} = 7 \pm 1$. The value of the link was since confirmed independently by a standard electrophoresis technique [1]. This gives us some confidence in the fitted linear regime. The extrapolated onset of crossing σ_0 is around 1/7.5 nm^2, about 0.4 of the surface charge $1/(2\pi l_B^2)$ corresponding to $\Xi = 1$ [dashed vertical line in Fig. 4(b)]. The largest measured value of n exceeds the theoretical maximum $|\mathrm{Lk}|$, which nonetheless is within the error bar. We may try to assess the effective (apparent) charge per unit length ρ. Assuming $l_t = 70$ nm and $S = 900$ nm we obtain $\rho \approx 1.4/l_B$, which matches our qualitative expectation. It is difficult for us to comment critically on the obtained value of ρ. In the better documented salty bulk solution case the effective charge of a rod is slowly increasing with the screening and is about $1.1/l_B$ for $\kappa R = 0.1$ and a nominal charge of $4/l_B$ [16]. At the interface counterions are massively released and replaced with the somewhat distant (as compared to charge regularization in the bulk) strong surface polarization. Also the high dielectric contrast at the interface should enhance the interaction.

Unfortunately, the expected decrease of n at the edge of the mean-field regime seems to occur at somewhat higher surface charge, where Ξ slightly exceeds unity. An upturn at high charge fraction seems observed. It is fair to say that the quality (homogeneity) of the bilayer deteriorates at these high charge densities. Also, we cannot exclude a slight systematic error in the estimated surface charge.

III. DISCUSSION OF SPECIFIC SURFACE EFFECTS

Some electrostatic effects known in the bulklike chain stiffening need to be reconsidered at the interface. Interfacial effects such as counterion release by a polyelectrolyte in the surface field need to be discussed. These effects were already introduced earlier but without a precise description.

A. Odijk stiffening

Repulsive intrachain interactions stiffen the filaments and enhance the apparent persistence length. Let us first consider the case of a quenched surface charge and no dielectric contrast. The tail of the interaction decays as $1/r^3$. Adapting the Odijk calculation [14] initially performed for a Yukawa potential, we find a logarithmic divergence of the internal interaction increase upon bending. For a filament of length S moderately curved in the plane of the substrate with uniform curvature C the interaction energy is increased by $\frac{l_B\rho^2\lambda^2 SC^2}{4}\ln[S/\lambda]$, which corresponds to an increase of the persistence length: $l_p = l_{p0} + \frac{l_B\rho^2\lambda^2}{2}\ln[S/\lambda]$. The apparent persistence length logarithmically depends on the filament size. Similarly, the persistence length should depend on the wave vector. In our case of (virtually infinite) periodic arrangements of crossings it is reasonable to use the distance between crossings instead of S under the logarithm. In the experimental range, the stiffening correction would go from negligible to order l_{p0}. At infinite

dielectric contrast the interaction decays as $1/r^5$ and there is no divergence anymore. Nonetheless, for finite dielectric contrast there is $1/r^3$ tail and hence a logarithmic divergence but with an amplitude divided by the dielectric contrast (about 80/5 in our case). Also, the surface charge is annealed in our case, which further divides the amplitude by 9. Altogether in the experiment the amplitude of the logarithm is weaker by about two orders of magnitude. The divergence is then pretty formal and the regular part of the stiffening correction buildup around $r \sim \lambda$ often dominates. This is much closer to Odijk's original result. It would be worthwhile to try to document the sensitivity of the stiffening to the boundary conditions. The calculation of stiffening is worth more precise consideration, even in the bulk case where the standard calculation does not rely on a perturbation of the newly obtained exact solution of the Poisson-Boltzmann equation.

B. Charge regularization

In the flat adsorbed structures considered, the two strands of the ply do not strongly interact except in the region close to crossings. Far from crossings, charge regularization takes place on the strands as on single (virtually infinite) strands. Charge regularization is hence ruled by self-energy, interaction with the unperturbed surface charge and counterion entropy. As compared to an isolated rod, the self-energy favors extra counterion condensation merely due to the image charge of the rod (remember, image charge has the same sign as the test charge). In contrast, the unperturbed interaction with the interface is repulsive for the counterions and favors counterion release. The case of an infinite rod has been considered in [32]. In the linear response, the self-energy (per unit length) is directly related to the Green's function $G(q,z=z_0)$ through $F_{\rm self} = \frac{1}{2}\rho^2 \int_0^\infty \frac{dq}{2\pi} G(q,z=z_0)$, where we took advantage of the fact that $G(q,z)$ also represents the potential created by an infinite rod lying parallel to the x axis at height z_0, $(x,0,z_0)$, with $\vec{q} = q\hat{y}$. The self-energy integral needs to be cut off at high momentum $q_c = 2\pi/R$. The self-energy diverges logarithmically at small distances from the surface merely due to the repulsion by the image charge. Formally, it overcomes the attraction $2\rho h/\lambda$ (per unit length) and the rod would stay a finite distance from the surface $h \sim l_B \rho \lambda$. On the other hand, the linear response is only exact when $l_B \rho \to 0$. For strongly charged rods the nonlinear Poisson-Boltzmann equation needs to be solved. In the case of annealed surface charge relevant for deposition on mixed bilayers, a strong attraction of surface charges under the rod (beyond linear response) occurs which essentially screens the rod from its image charge and also drastically reduces the interaction between charges on the rod. As a result, the system is dominated by the unperturbed interaction; we hence anticipate strong attraction between the rod and the bilayer and counterion release [32]. At crossings the two strands attract counterions and counterion release should not be complete. This effect slightly further favors direct contact between the rods. The interaction energy between projections at crossings preserves its functional form. Although counterions are released, they are replaced by the surface charge accumulated under the rod. The effective charge seen at large distances (as compared to the rod radius) should qualitatively be of order $1/l_B$ and could be roughly estimated from an Oosawa type of argument [37]. The value $\rho = 1.4/l_B$ obtained by fitting the data matches our expectations. Treating the interaction between projections this way is close in spirit to the often used DH asymptotics of the Poisson-Boltzmann solution in bulk.

C. Plasmid deposited onto a neutral substrate from salty solution

For a neutral surface, interfacial effects come only from the polarization of the salt solution and from the image charge. The self-energy per unit length obtained by integration of the Green's function $G(z,q)$ takes the form [Eq. (B3)]:

$$F_{\rm self} = \tfrac{1}{2} l_B \rho^2 \mathrm{K}_0(2\kappa h), \tag{9}$$

where K_0 is a modified Bessel function and the self-energy is set to zero infinitely away from the substrate. For a rod approaching the bilayer surface the self-energy diverges as $F_{\rm self} \sim \frac{1}{2} l_B \rho^2(-\Gamma - \ln \kappa h)$, where the reference is again taken infinitely away from the surface and Γ is the Euler constant. The logarithmically divergent repulsion at the surface must be overcome by a local short range attraction to ensure adsorption. Assuming some contact energy μ per unit filament length on the substrate strong enough to enforce contact between filaments at crossings leads to the penalty $F_h \sim \mu^{3/4} l_p^{1/4} R^{1/2}$, where a correction due to the self-energy has been neglected. The long range interactions between projected filaments near crossings contribute $F_{\rm int} = \rho^2 \frac{2\pi l_B}{\kappa \sin\theta}$ away from the surface and twice as much right at the surface. In the absence of surface charge the image charge induces extra counterion condensation and the effective charge of the plasmid should be somewhat weaker near the surface than in the far bulk salt solution. For the same effective linear charge the interaction between projections is thus the same as for a quenched surface charge, where λ is replaced by $\kappa^{-1}/2$ (away from the surface). Experiments [1] show that for the same number of crossings λ and κ^{-1} are proportional following roughly $\lambda = \kappa^{-1}/2$. One important difference between the two sets of experiments is that plasmids are less adsorbed on the neutral surface and rather float over the surface at an average height of 2–3 nm; the strict 2D nature of the conformations is not always obvious. For the same effective linear charge we would expect $\lambda/3 = \kappa^{-1}/2$ for an annealed surface charge in the linear approximation. The experimental result suggests that the effective plasmid charge on the charged surface is about $\sqrt{3}$ times that on the neutral surface. Given that in the former case there is counterion release and in the latter over condensation this seems reasonable. The comparison between deposition from a salt solution and onto a charged surface supports the general idea that the number of crossings is controlled by screened electrostatics.

IV. CONCLUSIONS

We discussed plasmids deposited from low salt solution onto oppositely charged surfaces. In all cases the plasmids were strongly adsorbed, lying flat on the surface almost everywhere. The electrostatic effects mainly provide attraction to the surface. The main motivations of our work are experiments where plasmids are deposited on mixed bilayers composed of cationic and neutral (yet zwitterionic) lipids. The very fact that

plasmids can be deposited on a bilayer composed of the neutral lipid only and also adopt flat configurations, demonstrates strong (short range) attraction between the plasmid and the neutral substrate. We considered two limiting cases: deposition on a charged substrate from salt free solution and deposition on a neutral substrate from salty solution. In the former case electrostatic is assumed to dominate the system while in the latter case a short range attraction is introduced. As the plasmids are flat on the surface in all cases examined, what remains to discuss is how the plasmids distribute their extra link between writhe and twist. Because the plasmids are flat almost everywhere but in very localized regions around crossings writhe is very simply linked to the number of crossings. Each crossing contributes one turn to the writhe and hence takes away one turn of twist. The situation here is much simpler than for 3D configurations deposited without strong adsorption (like on microscopy grids) where the writhe depends on geometrical details (for the simple case of a helical ply, on the helical angle). The number of crossings is obtained by balancing the spared elastic twist energy upon crossing and the interaction penalty at crossings. The penalty for crossing consists of two contributions which are counteracting upon increase of surface charge density. For moderate surface charge density, the far (mutual) interaction dominates and right angle crossings are expected. The number of crossings decreases linearly with the area per surface charge. For somewhat larger surface charge, a decrease of the number of crossings is imposed by the now dominating loss of interaction energy with the surface at the crossing. Eventually an upturn of the number of crossings is expected when most of the counterions of the bilayer condensate and the substrate turns into a highly screening two-dimensional plasma. All these regimes are observed in the experiments by some of us [1].

We provide some detailed calculations in the linear regime equivalent to a DH approximation within the ionic interfacial fluid. These are accurate for weakly charged molecules. Plasmids are strongly charged and, at the mean-field level, a full solution of the nonlinear Poisson-Boltzmann equation is required which is at least in part numerical. We only have very partial numerical solution of the relevant Poisson-Boltzmann equations.

Based on this and on qualitative arguments following Ref. [32], we assumed counterion release by the plasmid close to the substrate and calculated the short range penalty. Following [32], the charged plasmid is screened from its (equal sign) image charge by the surface charge which accumulates under it and the self-energy cancels to a large extent. These semiqualitative arguments use the notion of local screening which is not completely rigorous. This may affect quantitatively (but not qualitatively) the conclusions of Ref. [32], which we also used here. There is certainly room for a quantitative theory of the adsorption of strongly charged polyelectrolytes on an annealed substrate.

The far interaction is estimated from the tail of the actual interaction valid at distances larger than the dDNA radius R. This tail is following the law obtained from the linear theory but with a renormalized linear charge density. The renormalized charge density is expected to be of order $1/l_B$, but to date we are lacking a more precise estimate. Fitting the experiments we get $1.4/l_B$.

We also modeled the case of a salty solution facing a neutral interface. The repulsive self-energy cannot be avoided by a strong surface charge polarization. The plasmid is merely repelled by its image charge. A strong enough "short range" attraction is required for plasmid adsorption.

When the number of crossings is ruled by the far interaction at crossings there is an equivalence between bulk salt concentration and surface charge through $\kappa^{-1} = \alpha\lambda$ when the variation of the renormalized charges is neglected. Experiments suggest that $\alpha \approx 2$; the linear theory rather predicts $\alpha = 2/3$ (annealed) or $\alpha = 2$ (quenched). The surface charge being annealed, the deviation of α from $2/3$ may correspond to an effective plasmid charge at the charged bilayer (where there is counterion release) $\sqrt{3}$ times higher than on the neutral bilayer where there is overcondensation.

Throughout, our estimates and the experiments show quantitative agreement to some extent. Several reasons for some disagreement are discussed below.

The actual neutral bilayer is composed of zwitterionic lipids. The surface dipoles do organize/orient under the field of the plasmid leading to extra attraction. It may not be enough to describe this attraction by a contact interaction. We may try and write a theory for a neutral surface composed of surfactant with a finite separation between internal charges. We also should keep in mind that electrostatics is not always enough to explain the deposition mechanisms and the detailed chemistry plays a role [38].

We neglected thermal fluctuations of both the bilayer (as it is supported this seems fine) and the dDNA at short wavelength. Even for stiff strands some extra short range repulsion arises from the shape fluctuations normal to the bilayer. The case of two fluctuating surfaces/membranes was examined by Hed and Safran [39], who report "fusion" instabilities. Entropic loops larger than the persistence length, which are fluctuating by definition, were treated properly. Throughout we assumed the plasmid is forced to be in a flat configuration. We proceeded by assuming scale separation. In the experiment only l_p is larger (say by more than one order of magnitude) than the other length scales. As always, the weak coupling regime of the surface ($\Xi < 1$) is rather narrow in σ. In particular the domain where self-crossings are observed covers only a half of a decade of σ. In the experiment crossing of dDNA seems to occur with a decrease of total height, so likely either with interpenetration or the lower strand is pushed into or deforming the bilayer. In the case of interpenetration the crossing angle should be affected (prescribed), which seems not to be the case.

We essentially provide an approximate mean-field solution and an estimate of the interaction restricted to the lowest order in the coupling parameter. Some effects due to charge correlations, beyond our current approximation, may need to be considered. Mean field was worked out more carefully in somewhat simpler geometries by Fleck [40], who also examines fluctuation corrections on top of the mean field [41] for the counterion density and gives expressions for the self-energy and the effective pair potential. As to the self-energy and pair potential our approach carries the same physics. In a recent work Mamasakhlisov *et al.* [42] address surfaces with annealed/partially annealed charges and show that in the mean field charges are renormalized. Our approach is consistent

with [42] in the sense that we introduce an effective DNA charge density. New physics enters in the strong coupling limit, where attraction between like charged surfaces is predicted in some intermediate distance range, which is not possible within mean field. According to simulations [23], the minimal coupling parameter to get attraction is pretty large, close to ten for planar equally charged surfaces. In our experiment, strands cross each other at right angles and no signature of attraction between plasmid strands at crossings is observed.

Besides any approximation there is the question of whether the plasmid can equilibrate its shape in the experiment. There is clear evidence that the shape can fluctuate and the plasmid redistribute length between different loops. It is less clear whether after adsorption the plasmid can add or release crossings to equilibrate. There are only a few events recorded where a small loop stands out of the bilayer and could flip before (re-)adsorbing. This process could be helped by the existence of less-adsorbing bilayer patches. It is appealing to try to at least partially address the kinetics. This seems easier for plasmids deposited from salty solution on a neutral substrate (contact interactions and high salt). In the case of salt where supercoiled plasmid shapes are expected in solution, some slow degrees of freedom could be possibly tracked after plasmid adsorption.

The actual charged substrate is a bilayer containing a controlled fraction of cationic surfactants. DNA/lipid interaction was considered theoretically early by Dan [31] and Schiessel [43]. There are examples in the literature that cationic surfactants specifically interact with DNA and markedly increase its persistence length. In the experiment [1] an increase of apparent plasmid length by about 20% is measured only at a charged surfactant fraction of 50%. We do not have a clear evidence of surfactant DNA binding from experiments at lower charge fractions. Very recently another fascinating effect related to the very structure of dDNA was pointed out by the Toulouse group [44,45]. These authors show that the coupling of dDNA denaturation to curvature is relevant in 2D. Their theory explains the presence of sharp kinks localized at denaturation bubbles. Similar kinks are observed for dDNA glued on mica by multivalent cations [46]. Under conditions where the adsorbed plasmids can reshape and reach equilibrium the soft denaturation bubbles could take some link for free. The deposition mechanism considered in this work [1] is somewhat softer and sharp kinks are rare but still could be documented. For surface charges where crossings are reported sharp kinks were never seen. Under slightly different conditions it may be possible to demonstrate (anti)correlations between the number of kinks and the number of self-crossings. We may address kinked plasmid shapes in future work.

ACKNOWLEDGMENTS

This work is supported by National Research Foundation of Korea (NRF2008-314-C00155) and (NRF2008-531-C00030).

APPENDIX A: PENALTY FOR CROSSING

We derive the simple form of the interaction between two infinite rods located in the surface and cutting each other under an angle θ. Consider two lines (1) and (2) located in a plane directed by $\mathbf{u_1}$ and $\mathbf{u_2}$ with charge density $\rho\delta(\mathbf{r_1} - s\mathbf{u_1})$ and $\rho\delta(\mathbf{r_2} - t\mathbf{u_2})$, where s and t run over the reals, their crossing is located at $s = t = 0$. The lines interact with the potential $V(\mathbf{r_1} - \mathbf{r_2})$, which leads to the interaction energy $F_{\rm int} = \rho^2 \int_{-\infty}^{+\infty} V(s\mathbf{u_1} - t\mathbf{u_2})\mathrm{d}t\,\mathrm{d}s$; a change of variables yields the simple form $F_{\rm int} = (|\mathbf{u_1} \times \mathbf{u_2}|)^{-1} \int_{-\infty}^{+\infty} V(x,y)\mathrm{d}x\,\mathrm{d}y$. The interaction is hence given by the in-plane Fourier transform at $q = 0$ through

$$F_{\rm int} = \frac{V(q=0)}{\sin\theta}, \tag{A1}$$

where θ is the angle between the two lines.

APPENDIX B: EFFECTIVE INTERACTION—CALCULATION AND GREEN'S FUNCTION

In this section, we provide some detail on the Green's functions introduced in the main text for: (i) the case of a salty solution facing a substrate with low dielectric constant (formally set to zero), (ii) the case of 2D plasma on top of a low dielectric substrate, and (iii) the case of a charged surface facing a salt free solution.

1. Salty solution

We are going to solve for the Green's function $G(z,z_0,q)$ of the linearized Poisson-Boltzmann equation Fourier transformed with respect to the lateral position measured from the source located a height z_0 over the surface,

$$\left(-q^2 + \frac{\partial^2}{\partial z^2}\right) G(z,q) - \kappa^2 G(z,q) = -4\pi l_B \delta(z - z_0), \tag{B1}$$

where $\kappa^2 = 8\pi l_B c_s$. The boundary conditions are of von Neumann type at both boundaries $z = 0$ and $z = \infty$. The source imposes a discontinuity in the slope of $G(z,q)$ at $z = z_0$ whilst the Green's function itself is continuous.

The solution is of the form $G(z,q) = A\exp(-Qz)$ for $z > z_0$ and $G(z,q) = B\exp(-Qz) + C\exp(Qz)$ for $z < z_0$, where $Q = (q^2 + \kappa^2)^{1/2}$. The condition at the surface and the two conditions at z_0 determine the three integration constants, A,B,C, to be $B = C = \frac{2\pi l_B}{Q}\exp(-Qz_0)$, $A = \frac{2\pi l_B}{Q}(\exp(-Qz_0) + \exp(Qz_0))$. Specializing to the case where the source and the test point are at the same height, we obtain

$$G(z_0, q=0) = \frac{2\pi l_B}{\kappa}(1 + \exp(-2\kappa z_0)). \tag{B2}$$

For large DH length ($\kappa z_0 < 1$), the interaction reduces to $\frac{4\pi l_B}{\kappa}$. Note that the 2D integration of the bulk potential $\frac{l_B}{r}\exp(-\kappa r)$ leads to half that interaction and corresponds to the limit $z_0 \to \infty$ in Eq. (B2), as it should. It is easy to see that for $z = z_0 = 0$, the 2D Fourier transform inverts to $G(0,r) = 2l_B \exp[-\kappa r]/r$ twice the interaction infinitely away from the surface. There is no power law tail here.

The self-energy $F_{\rm self}$ can be obtained by integrating equal height Green's function $G(z = h, z_0 = h, q)$, $F_{\rm self} = \frac{1}{2}\rho^2 \int_0^\infty \frac{\mathrm{d}q}{2\pi} G(h,h,q)$. The related integral has a form of

modified Bessel function K_0,

$$\int_0^\infty \frac{2\pi}{(q^2+\kappa^2)}^{1/2} e^{-2h\sqrt{q^2+\kappa^2}} \frac{dq}{2\pi} = K_0(2\kappa h), \qquad \text{(B3)}$$

and we obtain $F_{\rm self} = \frac{1}{2} l_B \rho^2 K_0(2\kappa h)$.

2. Two-dimensional plasma

We now consider the instructive limiting case when all counterions are localized at but free to move in the surface. For convenience we consider a positive charge density σ_+ and a negative one $-\sigma_-$, both living at the surface. The total surface charge density is neutral on average. As above, a unit source charge is placed at a distance z_0 over the surface and polarizes the surface charge. Consistently with the general frame we treat the plasma in the DH approximation. Away from the surface there is no space charge (no salt) and the Green's function satisfies the Poisson equation $(-q^2 + \frac{\partial^2}{\partial z^2})G(z,q) = -4\pi l_B \delta(z - z_0)$. Since both charge distributions are assumed to follow Boltzmann's law, this sets the boundary condition at the surface: $\frac{\partial}{\partial z} G(z,q)|_{z=0} = 4\pi l_B(\langle\sigma_+ + \sigma_-\rangle)G(0,q)$, where the reference for G has been taken in the surface infinitely away from the source. The solution is of the form $G(z,q) = A\exp(-qz)$ for $z > z_0$ and $G(z,q) = B\exp(-qz) + C\exp(qz)$ for $z < z_0$. It is convenient to introduce a length $\lambda^\star = (2\pi l_B(\langle\sigma_+ + \sigma_-\rangle))^{-1}$ to obtain $C = 2\pi l_B \exp[-qz_0]/q$, $B = C(q\lambda^\star - 2)/(q\lambda^\star + 2)$, $A = B + 2\pi l_B \exp[qz_0]/q$. Specializing to $z = z_0 = 0$, we get the interaction

$$G(0,q=0) = 2\pi l_B \lambda^\star. \qquad \text{(B4)}$$

If the cations are not mobile in the surface we drop their concentration in $\lambda^\star$. Away from the surface when $z = z_0 \neq 0$ we get $G(z_0,q=0) = 2\pi l_B \lambda^\star(1 + 2z_0/\lambda^\star)$ to lowest order in $z_0/\lambda^\star$. The large r expansion of $G(z,r)$ shows the power law tail: $G(0,r) \sim \frac{l_B \lambda^{\star 2}}{2r^3}$.

3. Gouy-Chapman Layer

We now consider the case of a source immersed in the GC layer a distance z_0 away from the surface. The Green's function is calculated as a perturbation to the GC solution. Under this condition, the Green's function $G(z,q)$ obeys the equation

$$\left(-q^2 + \frac{\partial^2}{\partial z^2}\right) G(z,q) - \frac{2}{(z+\lambda)^2} G(z,q) = -4\pi l_B \delta(z - z_0). \qquad \text{(B5)}$$

This equation is supplemented with the von Neumann boundary condition at infinity and $\frac{\partial G(z,q)}{\partial z}|_0 = 0$ for quenched surface charge or $\frac{\partial G(z,q)}{\partial z}|_0 = 2G(0,q)/\lambda$ for annealed surface charge. The solution is of the form $G(z,q) = A\exp(-qz)(\frac{1}{z+\lambda} + q)$ for $z > z_0$ and $G(z,q) = B\exp(-qz)(\frac{1}{z+\lambda} + q) + C\exp(qz)(\frac{1}{z+\lambda} - q)$ for $z < z_0$. In the quenched case, $C = -2\pi l_B \frac{\exp(-qz_0)}{q^3}(\frac{1}{z_0+\lambda} + q)$, $B = 2\pi l_B \frac{\exp(-qz_0)}{q^3} \frac{1-q\lambda+q^2\lambda^2}{1+q\lambda+q^2\lambda^2}(\frac{1}{z_0+\lambda} + q)$, $A = B - 2\pi l_B \frac{\exp(qz_0)}{q^3}(\frac{1}{z_0+\lambda} - q)$. In the annealed case, $C = -2\pi l_B \frac{\exp(-qz_0)}{q^3}(\frac{1}{z_0+\lambda} + q)$, $B = 2\pi l_B \frac{\exp(-qz_0)}{q^3} \frac{3-3q\lambda+q^2\lambda^2}{3+3q\lambda+q^2\lambda^2}(\frac{1}{z_0+\lambda} + q)$, $A = B - 2\pi l_B \frac{\exp(qz_0)}{q^3}(\frac{1}{z_0+\lambda} - q)$. Specializing to the case $z = z_0 = 0$, we obtain the interaction $G^{q,a}(0,q=0)$ for annealed and quenched surface charge condition, respectively:

$$G^q(0,q=0) = 4\pi l_B \lambda, \quad G^a(0,q=0) = 4\pi l_B \lambda/3. \qquad \text{(B6)}$$

The results are consistent with the additivity of the polarizable surface densities in the interaction where a localized density contributes twice as much as a diffuse one. The power law tail of the Green's function follows from the low-q expansion as $G^a(0,r) \sim 2l_B\lambda^4/r^5$ and $G^q(0,r) \sim 18 l_B \lambda^4/r^5$. For two points at the same height slightly over the interface there is no generic $\sim 1/r^3$ tail. We do not give here the Green's function for finite dielectric contrast, which can be obtained following the same lines. In the latter case, there is a generic $\sim 1/r^3$ tail with an amplitude inversely proportional to the dielectric contrast ϵ_w/ϵ, $G^q(0,r) \sim 2(\epsilon/\epsilon_w) l_B \lambda^2/r^3$, $G^a(0,r) \sim \frac{2}{9}(\epsilon/\epsilon_w) l_B \lambda^2/r^3$. In the text we did not consider the finite contrast tail, with the noticeable exception of the electrostatic stiffening where it provides a logarithmic divergence of the persistence length; throughout this is a good approximation as long as distances larger than $\sqrt{\epsilon_w/\epsilon}\lambda$ do not matter. In our case $\epsilon \approx 5\epsilon_w/80$. The integrated interaction used in the main text is not affected by the finite dielectric contrast as both $G^q(0,q=0)$ and $G^a(0,q=0)$ are independent of the dielectric contrast.

APPENDIX C: MINIMIZATION OF FREE ENERGY AND SHAPE

To get more insight, subdominant energy terms have to be considered. There are mainly two of those, the bending energy in the adsorbed plasmid sections and the shape dependent correction to the intrastrand interaction energy beyond the straight crossing line approximation. The bending modulus includes electrostatic stiffening, which takes into account intrastrand interactions. The contribution of the stiffening to the energy and the intrastrand interaction have similar dependence on the GC length and strand length between crossings. Both these contributions become negligible at somewhat higher surface screening, corresponding to high number n of crossings separated by a strand length $l = S/(2n)$. In this regime, the bare stiffness prevails. We hence end up with one subdominant energy term $E_b = \frac{1}{2}\int_0^l \mathrm{d}s\, l_p(\frac{\mathrm{d}\theta_1(s)}{\mathrm{d}s})^2$ for strand (1) and similar for strand (2). At this level the crossing is a black box coupling to the flat strand (considered at larger scale only) by the boundary angle $\theta = \theta_1 - \theta_2$ at the crossing. We calculate the optimal shape of the loose surface ply by functional minimization. In the current approximation, we find that the shape is an arc of a circle. The total energy can be recast as

$$F = l_p \frac{\theta^2}{S/(2n)} + \frac{4\pi l_B \lambda}{3\sin\theta}. \qquad \text{(C1)}$$

The optimal angle obeys

$$\frac{\theta \sin\theta^2}{\cos\theta} = \frac{\rho^2}{6\sigma} \frac{S}{l_p n}. \qquad \text{(C2)}$$

This applies when the bending energy is larger than the thermal energy, which is typically for $n \geqslant 5$ in the experiment. In this

regime the angle θ is small and only weakly depends on n. For $\sigma l_B^2 \gg 1$, the surface charge is to be replaced by the constant $1/l_B^2$. The far field interaction between projected strands is then no longer dominating the penalty for crossing but still carries the angular dependence. Note that for small angles θ the leading penalties also acquire an angular dependence. The minimum curvature criterion to avoid wrapping becomes $h''(x=0) < \sin\theta^2/R$. Rather than wrapping, the strand may adopt the minimum curvature. The profile can then be solved without the condition $h''(\Lambda) = 0$ and F_h is now dependent on θ. The strands may also go out of contact at crossings and indeed the localized repulsive force arising from mutual interaction is to be divided by $\sin\theta$. Other solutions could also be considered. Nevertheless, these refinements rely on geometrical details too ill-controlled to be discussed here.

[1] T. Schmatko *et al*., e-print arXiv:1205.2991v1.
[2] A. V. Vologodskii and N. R. Cozzarelli, Annu. Rev. BioPhys. Biomol. Struct. **23**, 609 (1994).
[3] C. Bustamante, S. B. Smith, J. Liphardt, and D. Smith, Curr. Opin. Struct. Biol. **10**, 279 (2000).
[4] T. R. Strick, J.-F. Allemand, D. Bensimon, and V. Croquette, Biophys. J. **74**, 2016 (1998).
[5] M. A. Berger and C. Prior, J. Phys. A **39**, 8321 (2006).
[6] S. Neukirch, Phys. Rev. Lett. **93**, 198107 (2004).
[7] N. Clauvelin, B. Audoly, and S. Neukirch, Macromolecules **41**, 4479 (2008).
[8] C. Bouchiat and M. Mézard, Phys. Rev. Lett. **80**, 1556 (1998).
[9] V. Rosetto, Europhys. Lett. **69**, 142 (2005).
[10] Yu. S. Velichko, K. Yoshikawa, and A. R. Khokhlov, Biomacromolecules **1**, 459 (2000).
[11] V. Rosetto and A. C. Maggs, J. Chem. Phys. **118**, 9864 (2003).
[12] B. S. Fujimoto and J. M. Schurr, Biophys. J. **82**, 944 (2002).
[13] J. F. Marko and E. D. Siggia, Macromolecules **27**, 981 (1994).
[14] T. Odijk, J. Polym. Sci.: Polymer Physics Edition **15**, 477 (1977).
[15] N. Clauvelin, B. Audoly, and S. Neukirch, Biophys. J. **96**, 3716 (2009).
[16] E. Trizac and G. Téllez, Phys. Rev. Lett. **96**, 038302 (2006).
[17] T. C. Boles, J. H. White, and N. R. Cozzarelli, J. Mol. Biol. **213**, 931 (1990).
[18] J. M. Sperrazza, J. C. Register III, and J. Griffith, Gene **31**, 17 (1984).
[19] G. Witz, K. Rechendorff, J. Adamcik, and G. Dietler, Phys. Rev. Lett. **101**, 148103 (2008).
[20] T. Sakaue, G. Witz, G. Dietler, and H. Wada, Europhys. Lett. **91**, 68002 (2010).
[21] B. Jancovici, J. Stat. Phys. **28**, 43 (1982); **80**, 445 (1995).
[22] R. Netz and H. Orland, Eur. Phys. J. E **1**, 203 (2000).
[23] A. G. Moreira and R. R. Netz, Phys. Rev. Lett. **87**, 078301 (2001); Eur. Phys. J. E **8**, 33 (2002).
[24] L. Samaj and E. Trizac, Phys. Rev. Lett. **106**, 078301 (2011).
[25] A. Yu. Grosberg, T. T. Nguyen, and B. I. Shklovskii, Rev. Mod. Phys. **74**, 329 (2002).
[26] R. Messina, J. Phys.: Condens. Matter **23**, 199801 (2009).
[27] D. B. Lukatsky and S. A. Safran, Phys. Rev. E **60**, 5848 (1999); **63**, 011405 (2000).
[28] A. W. C. Lau, D. B. Lukatsky, P. Pincus, and S. A. Safran, Phys. Rev. E **65**, 051502 (2002).
[29] S. Safran, *Statistical Thermodynamics of Surfaces, Interfaces and Membranes, Frontiers in Physics* (Addison-Wesley, Reading, MA, 1994).
[30] Ye. Fang and J. Yang, J. Phys. Chem. B **101**, 441 (1997).
[31] N. Dan, Biophys. J. **73**, 1842 (1997).
[32] P. Sens and J.-F. Joanny, Phys. Rev. Lett. **84**, 4862 (2000).
[33] F. Brock Fuller, Proc. Natl. Acad. Sci. USA **75**, 3557 (1978).
[34] B. I. Shklovskii, Phys. Rev. E **60**, 5802 (1999).
[35] R. Metzler, A. Hanke, P. G. Dommersnes, Y. Kantor, and M. Kardar, Phys. Rev. Lett. **88**, 188101 (2002).
[36] B. Duplantier, J. Stat. Phys. **54**, 581 (1989).
[37] F. Oosawa, *Polyelectrolytes* (Dekker, New York, 1971).
[38] H. Boroudjerdi, Y. W. Kim, A. Naji, R. R. Netz, X. Schlagberger, and A. Serr, Phys. Rep. **416**, 129 (2005).
[39] G. Hed and S. A. Safran, Phys. Rev. Lett. **93**, 138101 (2004).
[40] C. C. Fleck and R. R. Netz, Biophys. J. **82**, 76 (2002).
[41] C. C. Fleck and R. R. Netz, Eur. Phys. J. E **22**, 261 (2007).
[42] Ye. S. Mamasakhlisov, A. Naji, and R. Podgornik, J. Stat. Phys. **133**, 659 (2008).
[43] H. Schiessel, Eur. Phys. J. B **6**, 373 (1998).
[44] J. Palmeri, M. Manghi, and N. Destainville, Phys. Rev. Lett. **99**, 088103 (2007).
[45] N. Destainville, M. Manghi, and J. Palmeri, Biophys. J. **96**, 4464 (2009).
[46] P. A. Wiggins, T. van der Heijden, F. Moreno-Herrero, A. Spakowitz, R. Phillips *et al*., Nat. Nanotech. **1**, 137 (2006).